Spectrochimica Acta, Vol. 45A, No. 2, pp. 271–279, 1989.
Printed in Great Britain.

0584–8539/89 $3.00+0.00

Vibrational force field and normal mode analysis of *N,N*-dimethylacetamide

ANIL M. DWIVEDI,* S. KRIMM* and SHEELLA MIERSON†

*Biophysics Research Division and Department of Physics, University of Michigan, Ann Arbor, MI 48109, U.S.A.; and †Department of Physiology, Medical College of Virginia, Virginia Commonwealth University, Richmond, VA 23298, U.S.A.

(*Received* 12 *August* 1988)

Abstract—A simple general valence force field has been refined for *N,N*-dimethylacetamide which includes both in-plane and out-of-plane modes. This force field gives good agreement between observed and calculated frequencies for this molecule and three of its deuterated derivatives, thus providing a good basis for the refinement of a force field for the imide group in polypeptides and proteins.

INTRODUCTION

Normal mode analyses of the vibrational spectra of polypeptides and proteins have been under development in our laboratory for a number of years [1]. We have refined transferable simple general valence force fields (SGVFF) for polypeptides containing the secondary amide group, starting from *N*-methylacetamide [2] and building up through known polypeptide structures such as polyglycine I [3–5], β-poly (L-alanine) [6, 7], and α-poly(L-alanine) [8, 9]. This work has made it possible to develop force fields that can account for the observed spectra of these molecules with an average discrepancy of $\sim 5\ cm^{-1}$ [10]. These force fields provide a basis for detailed interpretations of spectral data, facilitating the analyses of structures that sometimes cannot be probed by other techniques [11, 12].

Such vibrational analyses have not been available for polypeptides with tertiary amides because of the absence of a complete SGVFF for this group. We have therefore undertaken a study of *N,N*-dimethylacetamide (DMA), a simple molecule which provides a model for the tertiary amide group. Normal mode calculations and the spectral analysis of DMA should provide a force field for imide polypeptides which will fill the gap in the vibrational analysis of peptides and proteins.

Except for earlier work by one of us [13], all other normal model calculations on DMA [14–16] have been incomplete, in that they considered only the in-plane vibrations. Although we previously calculated both in-plane and out-of-plane modes [13], these results had two main problems: (1) the calculated values of the torsion modes did not agree with the observed frequencies, and (2) some of the force constants, for example CCO deformation, NCO deformation, and CCN deformation, had values which did not seem to be reasonable. In order to develop a force field for imide polypeptides comparable to that for amide polypeptides, we have therefore adopted a systematic approach and have tried to make the starting force field of the model (DMA) as good as possible. This has prompted us to reconsider the normal mode calculations of DMA and to refine its force field. The most common polypeptides containing imide groups are ones with proline residues. Similar to our earlier approach [1], we plan to use the DMA force field for normal mode calculations of several proline-containing peptides, adjusting the force constants where necessary to obtain a set for the prolyl group in the polypeptide chain.

In the present work an SGVFF for the DMA molecule has been refined. Far i.r. data (not reported earlier) and low frequency Raman modes have been used to adjust the torsion force constants. The assignments in this low frequency region are slightly different from those proposed previously [13]. This force field was used to calculate the normal modes of three deuterated derivatives of DMA, and the agreement between the calculated and observed values is quite good.

EXPERIMENTAL

Anhydrous *N,N*-dimethylacetamide was purchased from Aldrich Chemical Company. Fourier transform i.r. spectra were obtained using a BOMEM-DA3 i.r. spectrometer, holding the liquid film between two silver chloride windows for the mid i.r. region and between polyethylene windows for the far i.r. region. Raman spectra were recorded on a Spex 1403 laser Raman spectrometer. For the deuterated derivatives, $CD_3CO(CH_3)_2$ (D_3), $CH_3CO(CD_3)_2$ (D_6), and $CD_3CO(CD_3)_2$ (D_9), the i.r. and Raman frequencies are those reported by GARRIGOU-LAGRANGE *et al.* [16, 17].

NORMAL MODE CALCULATIONS

N,N-dimethylacetamide with C_s molecular symmetry (see Fig. 1) has 15 atoms, allowing a total of 39 normal modes of which 24 are planar (A') and 15 are non-planar (A''). All the modes are both Raman and i.r. active, but the modes that are strong in Raman and are polarized, generally belong to the A' symmetry species.

The molecular structure of DMA has not been determined experimentally. Previous authors

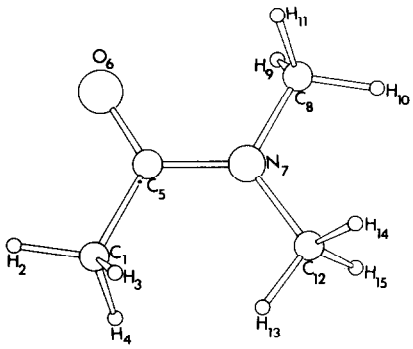

Fig. 1. Structure of *N*,*N*-dimethylacetamide molecule, with numbering of atoms.

[13–16] have calculated its normal modes assuming a structure similar to that of *N*-methylacetamide (NMA) and have used the NMA bond lengths and bond angles. For example, in our earlier calculation [13] the bond lengths and bond angles of crystalline NMA [18] were used. This may not be a good approximation since NMA molecules interact with each other via intermolecular hydrogen bonds whereas no such bonds exist in DMA. The best structural approximation should be provided by sarcosyl residues present in linear peptides. In the present calculation the bond lengths and bond angles for non-hydrogen atoms have been taken as the mean of the corresponding values present in three sarcosyl peptides [19, 20]. As in our earlier work [1], the C–H bond lengths in the methyl groups have been taken to be 1.09 Å and a tetrahedral geometry has been assumed around each methyl carbon. In agreement with an energy minimization calculation [21], the hydrogens of the methyl groups are staggered and the in-plane hydrogen of the carbon methyl group is directed essentially parallel to the C–N bond. The bond lengths and bond angles used in our calculations are listed in Table 1.

A total of 45 internal coordinates were defined, and are listed in Table 2. Excluding angular redundancies, 40 local symmetry coordinates were defined and are listed in Table 3. Because of the non-equal lengths of the N_7–C_8 and N_7–C_{12} bonds, we have not combined the respective out-of-plane angle bends into one symmetry coordinate; nevertheless, they are highly coupled with each other and give rise to only one normal mode in which C_8 and C_{12} move together along the same direction.

As a starting point for the calculation, we transferred all the force constants from [13]. This gave quite reasonable agreement with the observed values for all the in-plane modes but the agreement was poor for out-of-plane modes. Far i.r. data were very helpful in the assignment of the low frequency out-of-plane modes and their corresponding force constants; after adjusting these, only minor changes were required in the in-plane force constants. Subsequently, this refined force field was used to compute the frequencies of the deuterated derivatives.

Our force field for DMA is listed in Table 4. Some of its main features are the following. The values of f(CCO), f(NCO), and f(CCN) have changed compared to [13], and their respective values of 1.606, 1.906 and 1.333 mdynes are now of the same order of magnitude as in our force fields for polypeptides [5, 7, 9, 12]. The force constants f(CO ob), f(NC_t ob) = f(NC_c ob), fCN t), f(CC t), f(NC_t t), f(NC_c t), f(CO ob, CN t), and f(NC_c ob, CN t) = f(NC_t ob, CN t) are also quite close to corresponding force constants in β-poly(L-alanine) [7], and the resulting predictions of the torsion and the C=O and N–CH_3 out-of-plane modes are very satisfactory. The angle bend force constants associated with the CH_3 groups bonded to N are different from those of the CH_3 group bonded to C, suggesting different environments. Other authors [13–16] have also found such differences. The closer proximity of C_8 to O (*cis* configuration, at a distance of 2.69 Å) compared with C_{12} (*trans* to O, at a distance of 3.6 Å) is reflected in the force constants f(NCO, CNC_c) and f(NCO, CNC_t): the former has a value of 0.6 mdyne whereas the latter is zero. The closeness of the O also seems to affect the interaction of f(CCO)

Table 1. Bond lengths and bond angles of *N*,*N*-dimethylacetamide used in our calculations

Bond	Value (Å)	Angle	Value (°)
C_1–C_5	1.524	C_1–C_5–O_6	120.55
C_5–O_6	1.227	C_1–C_5–N	118.4
C_5–N_7	1.344	O_6–C_5–N_7	121.05
N_7–C_8	1.446	C_5–N_7–C_8	118.8
N_7–C_{12}	1.460	C_5–N_7–C_{12}	124.9
C_1–H_2		C_8–N_7–C_{12}	116.3
C_1–H_3		Angles at C_1, C_8 and C_{12}	109.47
C_1–H_4			
C_8–H_9	1.09		
C_8–H_{10}			
C_8–H_{11}			
C_{12}–H_{13}			
C_{12}–H_{14}			
C_{12}–H_{15}			

Table 2. Internal coordinates of *N,N*-dimethylacetamide*

$R_1 = \Delta r(C_1-C_5)$	C–C stretch
$R_2 = \Delta r(C_5-O_6)$	C–O stretch
$R_3 = \Delta r(C_5-N_7)$	C–N stretch
$R_4 = \Delta r(N_7-C_8)$	N–C_c stretch
$R_5 = \Delta r(N_7-C_{12})$	N–C_t stretch
$R_6 = \Delta r(C_1-H_2)$	C–H stretch
$R_7 = \Delta r(C_1-H_3)$	C–H stretch
$R_8 = \Delta r(C_1-H_4)$	C–H stretch
$R_9 = \Delta r(C_8-H_{10})$	C_c–H stretch
$R_{10} = \Delta r(C_8-H_9)$	C_c–H stretch
$R_{11} = \Delta r(C_8-H_{11})$	C_c–H stretch
$R_{12} = \Delta r(C_{12}-H_{13})$	C_t–H stretch
$R_{13} = \Delta r(C_{12}-H_{14})$	C_t–H stretch
$R_{14} = \Delta r(C_{12}-H_{15})$	C_t–H stretch
$R_{15} = \Delta\theta(C_1-C_5-O_6)$	C–C–O bend
$R_{16} = \Delta\theta(C_1-C_5-N_7)$	C–C–N bend
$R_{17} = \Delta\theta(N_7-C_5-O_6)$	N–C–O bend
$R_{18} = \Delta\theta(C_5-N_7-C_8)$	C–N–C_c bend
$R_{19} = \Delta\theta(C_5-N_7-C_{12})$	C–N–C_t bend
$R_{20} = \Delta\theta(C_8-N_7-C_{12})$	C_c–N–C_t bend
$R_{21} = \Delta\theta(C_5-C_1-H_2)$	C–C–H bend
$R_{22} = \Delta\theta(C_5-C_1-H_3)$	C–C–H bend
$R_{23} = \Delta\theta(C_5-C_1-H_4)$	C–C–H bend
$R_{24} = \Delta\theta(H_2-C_1-H_3)$	H–C–H bend
$R_{25} = \Delta\theta(H_2-C_1-H_4)$	H–C–H bend
$R_{26} = \Delta\theta(H_3-C_1-H_4)$	H–C–H bend
$R_{27} = \Delta\theta(N_7-C_8-H_{10})$	N–C_c–H bend
$R_{28} = \Delta\theta(N_7-C_8-H_9)$	N–C_c–H bend
$R_{29} = \Delta\theta(N_7-C_8-H_{11})$	N–C_c–H bend
$R_{30} = \Delta\theta(H_{10}-C_8-H_9)$	H–C_c–H bend
$R_{31} = \Delta\theta(H_{10}-C_8-H_{11})$	H–C_c–H bend
$R_{32} = \Delta\theta(H_9-C_8-H_{11})$	H–C_c–H bend
$R_{33} = \Delta\theta(N_7-C_{12}-H_{13})$	N–C_t–H bend
$R_{34} = \Delta\theta(N_7-C_{12}-H_{14})$	N–C_t–H bend
$R_{35} = \Delta\theta(N_7-C_{12}-H_{15})$	N–C_t–H bend
$R_{36} = \Delta\theta(H_{13}-C_{12}-H_{14})$	H–C_t–H bend
$R_{37} = \Delta\theta(H_{13}-C_{12}-H_{15})$	H–C_t–H bend
$R_{38} = \Delta\theta(H_{14}-C_{12}-H_{15})$	H–C_t–H bend
$R_{39} = \Delta\omega(C_5-O_6 \begin{smallmatrix} C_1 \\ N_7 \end{smallmatrix})$	C–O out-of-plane bend
$R_{40} = \Delta\omega(N_7-C_{12} \begin{smallmatrix} C_8 \\ C_5 \end{smallmatrix})$	N–C_t out-of-plane bend
$R_{41} = \Delta\omega(N_7-C_8 \begin{smallmatrix} C_5 \\ C_{12} \end{smallmatrix})$	N–C_c out-of-plane bend
$R_{42} = \Delta\tau(C_1-C_5) = [\Delta\tau(H_2C_1C_5O_6) + \Delta\tau(H_3C_1C_5O_6) + \Delta\tau(H_4C_1C_5O_6) + \Delta\tau(H_2C_1C_5N_7) + \Delta\tau(H_3C_1C_5N_7) + \Delta\tau(H_4C_1C_5N_7)]/6$	C–C torsion
$R_{43} = \Delta\tau(C_5-N_7) = [\Delta\tau(C_1C_5N_7C_8) + \Delta\tau(O_6C_5N_7C_8) + \Delta\tau(C_1C_5N_7C_{12}) + \Delta\tau(O_6C_5N_7C_{12})]/4$	C–N torsion
$R_{44} = \Delta\tau(N_7-C_8) = [\Delta\tau(C_5N_7C_8H_9) + \Delta\tau(C_5N_7C_8H_{10}) + \Delta\tau(C_5N_7C_8H_{11}) + \Delta\tau(C_{12}N_7C_8H_9) + \Delta\tau(C_{12}N_7C_8H_{10}) + + \Delta\tau(C_{12}N_7C_8H_{11})]/6$	N–C_c torsion
$R_{45} = \Delta\tau(N_7-C_{12}) = [\Delta\tau(C_5N_7C_{12}H_{13}) + \Delta\tau(C_5N_7C_{12}H_{14}) + \Delta\tau(C_5N_7C_{12}H_{15}) + \Delta\tau(C_8N_7C_{12}H_{13}) + \Delta\tau(C_8N_7C_{12}H_{14}) + \Delta\tau(C_8N_7C_{12}H_{15})]/6$	N–C_t torsion

*C_c: methyl carbon *cis* to oxygen. C_t: methyl carbon *trans* to oxygen.

Table 3. Symmetry coordinates of *N,N*-dimethylacetamide*

In-plane	
$S_1 = R_1$	CC s
$S_2 = R_2$	CO s
$S_3 = R_3$	CN s
$S_4 = R_4$	NC_c s
$S_5 = R_5$	NC_t s
$S_6 = (R_6 + R_7 + R_8)/3^{1/2}$	CH_3 ss
$S_7 = (2R_6 - R_7 - R_8)/6^{1/2}$	CH_3 as
$S_8 = (R_9 + R_{10} + R_{11})/3^{1/2}$	C_cH_3 ss
$S_9 = (2R_9 - R_{10} - R_{11})/6^{1/2}$	C_cH_3 as
$S_{10} = (R_{12} + R_{13} + R_{14})/3^{1/2}$	C_tH_3 ss
$S_{11} = (2R_{12} - R_{13} - R_{14})/6^{1/2}$	C_tH_3 as
$S_{12} = (2R_{16} - R_{15} - R_{17})/6^{1/2}$	CCN d
$S_{13} = (R_{15} - R_{17})/2^{1/2}$	CO ib
$S_{14} = (2R_{20} - R_{18} - R_{19})/6^{1/2}$	C_tNC_c d
$S_{15} = (R_{18} - R_{19})/2^{1/2}$	C_tNC_c r
$S_{16} = (R_{24} + R_{25} + R_{26} - R_{21} - R_{22} - R_{23})/6^{1/2}$	CH_3 sb
$S_{17} = (2R_{26} - R_{24} - R_{25})/6^{1/2}$	CH_3 ab
$S_{18} = (2R_{21} - R_{22} - R_{23})/6^{1/2}$	CH_3 r
$S_{19} = (R_{30} + R_{31} + R_{32} - R_{27} - R_{28} - R_{29})/6^{1/2}$	C_cH_3 sb
$S_{20} = (2R_{32} - R_{30} - R_{31})/6^{1/2}$	C_cH_3 ab
$S_{21} = (2R_{27} - R_{28} - R_{29})/6^{1/2}$	C_cH_3 r
$S_{22} = (R_{36} + R_{37} + R_{38} - R_{33} - R_{34} - R_{35})/6^{1/2}$	C_tH_3 sb
$S_{23} = (2R_{38} - R_{36} - R_{37})/6^{1/2}$	C_tH_3 ab
$S_{24} = (2R_{33} - R_{34} - R_{35})/6^{1/2}$	C_tH_3 r
Out-of-plane	
$S_{25} = (R_7 - R_8)/2^{1/2}$	CH_3 as
$S_{26} = (R_{10} - R_{11})/2^{1/2}$	C_cH_3 as
$S_{27} = (R_{13} - R_{14})/2^{1/2}$	C_tH_3 as
$S_{28} = (R_{24} - R_{25})/2^{1/2}$	CH_3 ab
$S_{29} = (R_{22} - R_{23})/2^{1/2}$	CH_3 r
$S_{30} = (R_{30} - R_{31})/2^{1/2}$	C_cH_3 ab
$S_{31} = (R_{28} - R_{29})/2^{1/2}$	C_cH_3 r
$S_{32} = (R_{36} - R_{37})/2^{1/2}$	C_tH_3 ab
$S_{33} = (R_{34} - R_{35})/2^{1/2}$	C_tH_3 r
$S_{34} = R_{39}$	CO ob
$S_{35} = R_{40}$	NC_t ob
$S_{36} = R_{41}$	NC_c ob
$S_{37} = R_{42}$	CC t
$S_{38} = R_{43}$	CN t
$S_{39} = R_{44}$	NC_c t
$S_{40} = R_{45}$	NC_t t

*s = stretch; ss = symmetric stretch; as = antisymmetric stretch; sb = symmetric bend; ab = antisymmetric bend; d = deformation; ib = in-plane bend; ob = out-of-plane bend; r = rock; t = torsion.

with the angle bends containing the methyl hydrogens. Of all the possible CCO, CCH or NCO, NCH types of interactions, only f(CCO, CCH_c) (force constant No. 49 in Table 4) has a non-zero value, −0.100, others being zero. It should be noted that H_c is the closest to O (2.51 Å). The refinement of the force field in the presence of interactions such as f(NCO, CNC_c) and f(CCO, CCH_c), not present in our previous peptide force fields [5, 7, 9, 12], introduces a new force constant f(CCN, CCO) in the DMA force field, again absent in the peptide force fields. Such an interaction has been reported in *ab initio* studies of the force fields of amides [22] and peptides [23].

RESULTS AND DISCUSSION

The calculated and observed frequencies of DMA and its three deuterated derivatives are listed in Table 5. All the i.r. and Raman frequencies for DMA are from our experiments, except for the 1661 (i.r.) and 1660 (Raman) cm^{-1} bands which are taken from [17]. These values are from the spectrum recorded in very dilute carbon tetrachloride solution to avoid molecular association, which influences the C=O stretch frequencies. The observed frequencies of the deuterated derivatives are taken from [17].

$CH_3CON(CH_3)_2$ (D_0)

The spectral region above 2000 cm^{-1} is quite complex because of the presence of Fermi resonance as well as combination and overtone bands, and therefore it is difficult to assign directly all the bands in this region. The i.r. spectrum shows four bands, at 3015, 2932, 2870 and 2815 cm^{-1}, whereas six bands are observed in Raman, at 3016, 2974, 2950, 2933, 2870 and 2815 cm^{-1}. The four Raman bands observed at 3016, 2974, 2950 and 2933 arise from Fermi resonance between fundamentals and combinations or overtones. A Fermi resonance analysis [24] for the observed 3016, 2974 pair, with intensity ratio $I(3016)/I(2974) \sim 0.574$, gives unperturbed values of 2989 and 3001 cm^{-1} for the corresponding fundamental and the overtone. This overtone could arise from the fundamental observed at 1497 cm^{-1} (A') in the Raman and assigned to the CH_3 antisymmetric bend (ab) mode of the methyl groups attached to the nitrogen atom. A similar analysis for the 2950, 2933 pair, with intensity ratio $I(2950)/I(2933) \sim 0.475$, gives unperturbed values of 2938 and 2944 cm^{-1} for the corresponding fundamental and the combination. In this case the combination may be due to CH_3 ab modes at 1479 cm^{-1} (calculated, A') and 1452 cm^{-1} (observed, A'). The remaining two bands at 2870 and 2815 cm^{-1} are most likely the overtones of the fundamentals observed at 1435 and 1413 cm^{-1}, respectively. Thus, of all the bands observed in this region only two, corresponding to CH_3 symmetric (ss) and antisymmetric (as) stretch, are fundamentals.

In addition to the imide I mode at 1660 cm^{-1}, which is mainly a combination of CO and CN stretch (s), the spectral region between 1700 and 950 cm^{-1} is largely dominated by the methyl group frequencies. The usual amide II band (NH in-plane-bend (ib) + CN s) in the 1560–1520 cm^{-1} region for peptides [1] is not (nor is expected to be) observed in DMA, but imide II (essentially CN s) should be seen, probably below 1460 cm^{-1} [1]. Interestingly, CN s mixes heavily with the CH_3 ab of the CH_3(N) groups, resulting in calculated modes at 1497 and 1453 cm^{-1}. These have contributions of 12 and 17%, respectively, from CN s and are in good agreement with the observed values. The other CH_3(N) ab modes are calculated at 1479 (A''), 1481 (A'') and 1474 (A''), but are not observed experimentally. The CH_3(C) ab modes are calculated at lower frequencies, the Raman band observed at 1435 cm^{-1} being assigned to these modes. Unlike the CH_3(N) groups, only a small splitting (2 cm^{-1}) is predicted for the CH_3(C) ab modes, con-

Table 4. Force constants for *N,N*-dimethylacetamide

Force constant*	Value†	Force constant*	Value†
1. f(CC)	4.134	31. f(CN, NC_c)	0.550
2. f(CN)	5.691	32. f(CN, NC_t)	0.550
3. f(CO)	9.700	33. f(CH, CH)	0.080
4. f(NC_t)	4.950	34. f(C_cH, C_cH)	0.080
5. f(NC_c)	4.950	35. f(C_tH, C_tH)	0.080
6. f(CH)	4.800	36. f(CC, CCO)	0.300
7. f(C_cH)	4.800	37. f(CC, CCN)	0.200
8. f(C_tH)	4.800	38. f(CC, CCH)	0.295
9. f(CCO)	1.606	39. f(CO, CCO)	0.450
10. f(CCN)	1.333	40. f(CO, NCO)	0.450
11. f(NCO)	1.906	41. f(CN, CCN)	0.511
12. f(CNC_c)	0.970	42. f(CN, NCO)	0.421
13. f(CNC_t)	0.970	43. f(CN, CNC_c)	0.100
14. f(C_cNC_t)	1.430	44. f(CN, CNC_t)	0.100
15. f(CCH)	0.657	45. f(NC_c, CNC_c)	0.400
16. f(HCH)	0.513	46. f(NC_c, NC_cH)	0.370
17. f(NC_cH)	0.785	47. f(NC_t, CNC_t)	0.400
18. f(HC_cH)	0.536	48. f(NC_t, NC_tH)	0.370
19. f(NC_tH)	0.785	49. f(CCO, CCH_c)	−0.100
20. f(HC_tH)	0.536	50. f(CCO, CCN)	0.280
21. f(CO ob)	0.548	51. f(CCN, CNC_c)	0.766
22. f(NC_c ob)	0.162	52. f(CCN, CNC_t)	0.766
23. f(NC_t ob)	0.162	53. f(NCO, CNC_c)	0.600
24. f(CC t)	0.100	54. f(CNC_c, CNC_t)	0.100
25. f(CN t)	0.680	55. f(CCH, CCH)	−0.012
26. f(NC_c t)	0.100	56. f(NC_cH, NC_cH)	−0.049
27. f(NC_t t)	0.100	57. f(NC_tH, NC_tH)	−0.049
28. f(CC, CN)	0.300	58. f(CO ob, CN t)	0.0111
29. f(CC, CO)	0.500	59. f(NC_c ob, CN t)	−0.070
30. f(CO, CN)	0.500	60. f(NC_t ob, CN t)	−0.070

*AB = AB bond stretch; ABC = ABC angle bend; X, Y = XY interaction; ob = out-of-plane angle bend; t = torsion; subscripts *t* and *c* denote the methyl carbons attached to N in *trans* and *cis* configurations with respect to O; subscript *c* to H (No. 49) denotes H attached to C is in *cis* configuration with respect to O.

†Units: mdyne/Å for stretch and stretch, stretch constants; mdyne for stretch, bend constants; and mdyne Å for all others.

sistent with only one band being observed. The large splitting of the CH_3(N) ab modes is mainly due to the interaction of CN s with CH_3(N) ab, such interactions being absent for the CH_3(C) group. A similar interaction was predicted by earlier normal mode calculations [13, 16]. Although the band observed at about 1268 cm^{-1} has been assigned as imide III [13], it really is not a counterpart of amide III in polypeptides, which consists mainly of NH ib, often with a CN s contribution. If we retain the imide III designation for DMA, it should be understood that this mode is mainly a characteristic antisymmetric stretch of the two N–CH_3 bonds. The two bands observed at about 1190 and 1180 cm^{-1} are assigned to in-plane CH_3(N) rock (r) mixed with skeletal stretches and to out-of-plane CH_3(C) r mixed with out-of-plane CH_3(N) r, respectively. Although these assignments are similar to earlier ones [13], the agreement between the calculated and observed values is better in the present calculation. Likewise, an out-of-plane CH_3 r mode observed at 1108 cm^{-1}, is predicted more accurately by our present calculation. The remaining bands observed in this region, at 1064, 1036, 1013 and 960 cm^{-1}, are in good agreement with the calculated values.

Bands in the region below 800 cm^{-1} are predominantly due to skeletal in-plane bend, out-of-plane bend and torsion vibrations. The strongest, and highly polarized, band in the Raman, at 737 cm^{-1}, is assigned to skeletal stretches belonging to the *A'* symmetry species. The mode observed at 598 cm^{-1} only in the i.r. is assigned to CO out-of-plane bend (ob) and is calculated at 602 cm^{-1}. A comparison with the results on NMA and other peptides [1] suggests that ~600 cm^{-1} is the right region for this mode, and that an earlier value of ~400 cm^{-1} [13] is too low. The imide IV mode (mainly CO ib) is calculated and observed at ~590 cm^{-1}, which is in agreement with the value computed earlier [13]. The other skeletal in-plane bend and rock modes, observed at 472, 420 and 262 cm^{-1}, are also satisfactorily predicted by our calculation and assigned as before [13]. The major differences between the present and earlier calculations are for the *A''* skeletal torsion modes. The N–C_c, N–C_t, and C–C (essentially methyl) torsions (t) are likely to be observed near 230 cm^{-1}, as our

Table 5. Calculated and observed frequencies (in cm^{-1}) of *N,N*-dimethyl acetamide and deuterated derivatives

Observed* i.r.	Observed* Raman	Calculated *A'*	Calculated *A''*	Potential energy distribution†
				$CH_3CON(CH_3)_2$ (D_0)
		2986		C_cH_3 as(45), C_tH_3 as(41), CH_3 as(12)
2989 w‡	2989 w‡	2981		CH_3 as(87)
		2981		C_cH_3 as(50), C_tH_3 as(49)
			2981	C_tH_3 as(91)
			2980	C_cH_3 as(96)
			2979	CH_3 as(88)
		2931		C_cH_3 ss(53), C_tH_3 ss(46)
2938 m‡	2938 s‡	2931		C_tH_3 ss(53), C_cH_3 ss(46)
		2930		CH_3 ss(99)
1661 s	1660 s	1660		CO s(71), CN s(17), CCN d(11)
1504 m	1497 w, sh	1497		C_tH_3 ab(28), C_cH_3 ab(15), C_tH_3 r(14), CN s(12)
			1481	C_cH_3 ab(42), C_tH_3 ab(41)
		1479		C_cH_3 ab(54), C_tH_3 ab(29), C_cH_3 r(10)
			1474	C_tH_3 ab(44), C_cH_3 ab(43)
1452 w	1452 m	1453		C_tH_3 ab(29), CN s(17), C_cH_3 ab(14), CO ib(11)
			1432	CH_3 ab(91)
	1435 m	1430		CH_3 ab(89)
1415 m	1413 s	1405		C_tH_3 sb(72), C_cH_3 sb(30)
1398 s	1396 m, sh	1399		C_cH_3 sb(68), C_tH_3 sb(31)
1358 m	1358 w	1361		CH_3 sb(95)
1269 m	1267 w	1274		NC_t s(37), C_cH_3 r(18), NC_c s(16), CO ib(13), C_tNC_c r(10)
1190 m	1189 w	1199		C_tH_3 r(32), NC_c s(19), CC s(17), CO ib(12)
1180 w	1179 w		1175	C_tH_3 r(41), C_cH_3 r(31)
	1108 vw		1104	C_cH_3 r(46), C_tH_3 r(40)
1064 w	1063 w	1072		C_cH_3 r(38), C_tH_3 r(24), NC_c s(14), NC_t s(14)
1036 w			1045	CH_3 r(83)
1014 m	1013 m	1004		CH_3 r(64)
960 vw	959 s	963		NC_c s(28), C_tH_3 r(16), C_cH_3 r(12), CC s(12)
737 vw	737 vs	731		CC s(27), NC_t s(19), NC_c s(13), CN s(13)
598 w			602	CO ob(73)
590 m	590 s	596		CO ib(49), CC s(17), NC_t s(13)
472 m	472 m	467		CCN d(53), C_tNC_c r(25), CO ib(11)
420 w	421 s	416		C_tNC_c d(82), CN s(16)
333 w			329	NC_c ob(23), NC_t ob(23), CO ob(13), CN t(13), CC t(10)
	262 w	259		C_tNC_c r(62), CCN d(35)
	240 w		237	NC_t t(91)
			236	NC_c t(67), CC t(31)
229 w			223	CC t(58), NC_c t(28)
	186 w		182	CN t(90), NC_t ob(16), NC_c ob(16)
				$CD_3CON(CH_3)_2$ (D_3)
		2985		C_cH_3 as(51), C_tH_3 as(48)
2989 w‡	2989 w‡	2981		C_tH_3 as(52), C_cH_3 as(48)
			2981	C_tH_3 as(99)
			2980	C_cH_3 as(99)
		2935		C_tH_3 ss(53), C_cH_3 ss(47)
2938 s‡	2938 s‡	2935		C_cH_3 ss(53), C_tH_3 ss(47)
2257 w	2260 m	2229		CD_3 as(97)
			2222	CD_3 as(98)
2155 w	2157 s	2112		CD_3 ss(98)
1650 s	1649 sh	1653		CO s(73), CN s(18), CCN d(11)
1500 m	1500 sh	1494		C_tH_3 ab(32), C_cH_3 ab(18), C_tH_3 r(15), CN s(10)
			1481	C_cH_3 ab(42), C_tH_3 ab(41)
		1479		C_cH_3 ab(53), C_tH_3 ab(30), C_cH_3 r(10)
1460 w			1474	C_tH_3 ab(44), C_cH_3 ab(43)
	1451 s	1445		C_tH_3 ab(24), CN s(21), C_cH_3 ab(13), CO ib(12), CC s(10)
1410 sh	1411 s	1405		C_tH_3 sb(77), C_cH_3 sb(26)
1398 s	1394 m	1397		C_cH_3 sb(70), C_tH_3 sb(27)
1276 m	1277 w	1274		NC_t s(38), C_cH_3 r(18), NC_c s(17), CO ib(13), C_tNC_c r(10)
1191 m	1190 w	1190		C_tH_3 r(35), CC s(19), NC_c s(17), CO ib(14)
			1175	C_tH_3 r(41), C_cH_3 r(37)
			1104	C_cH_3 r(46), C_tH_3 r(41)
	1071 vw	1071		C_cH_3 r(37), C_tH_3 r(23), NC_c s(14), NC_t s(14)
1058 w	1052 w	1061		CD_3 sb(88), CC s(15)
	1038 w	1029		CD_3 ab(94)
	1018 vw		1028	CD_3 ab(95)
	954 s	961		NC_c s(31), C_tH_3 r(18), NC_t s(14), C_cH_3 r(14)

Table 5. (*continued*)

Observed* i.r.	Observed* Raman	Calculated *A'*	Calculated *A''*	Potential energy distribution†
852 vw	853 w		854	CD_3 r(71), CO ob(22)
826 w	825 vs	813		CD_3 r(57), CCN d(10)
700 vw	700 vs	686		NC_t s(20), CN s(18), CD_3 r(18), NC_c s(12), CC s(11)
567 m	568 s	571		CO ib(48), CC s(24)
			555	CO ob(56), CD_3 r(23)
447 vs	445 w	438		CCN d(44), C_tNC_c r(35), CD_3 r(10)
410 vw	408 s	415		C_tNC_c d(81), CN s(18)
318 w			326	NC_c ob(24), NC_t ob(24), CO ob(14), CN t(14)
		244		C_tNC_c r(54), CCN d(42)
			236	NC_t t(91)
			232	NC_c t(92)
			174	CN t(86), NC_t ob(17), NC_c ob(17)
			164	CC t(93)
				$CH_3CON(CD_3)_2$ (D_6)
2989 w‡	2989 w‡	2982		CH_3 as(99)
			2980	CH_3 as(99)
2938 w‡	2938 s‡	2934		CH_3 ss(100)
2263 w	2264 w	2239		C_cD_3 as(51), C_tD_3 as(45)
		2226		C_tD_3 as(52), C_cD_3 as(46)
			2225	C_tD_3 as(94)
			2224	C_cD_3 as(94)
		2115		C_tD_3 ss(50), C_cD_3 ss(48)
2140 w	2142 s	2114		C_cD_3 ss(51), C_tD_3 ss(48)
1654 s	1645 sh	1656		CO s(74), CN s(16), CCN d(11)
1439 sh	1449 s	1450		CN s(33), CO ib(20), CC s(12)
	1431 m		1432	CH_3 ab(91)
1422 s		1428		CH_3 ab(86)
1358 m	1360 w	1357		CH_3 sb(95), CC s(12)
1247 m	1247 w	1242		NC_t s(56), NC_c s(18), C_tNC_c r(10)
1144 w	1144 w	1155		NC_c s(44), C_cD_3 sb(23), CC s(14), CO ib(10)
1065 vw	1067 m	1072		C_tD_3 sb(87)
			1062	C_cD_3 ab(41), C_tD_3 ab(28), C_cD_3 r(10)
		1062		C_tD_3 ab(47), C_cD_3 sb(18), C_cD_3 ab(17)
		1056		C_cD_3 ab(63), C_cD_3 sb(26)
1055 vw			1054	C_tD_3 ab(59), C_cD_3 ab(31)
		1049		C_tD_3 ab(46), C_cD_3 sb(24), C_cD_3 ab(11)
1034 vw			1048	CH_3 r(69), C_cD_3 ab(16)
976 m	977 s	990		CH_3 r(57), CC s(13)
			946	C_tD_3 r(38), C_cD_3 r(33)
	878 w			?
840 vw	841 m		842	C_cD_3 r(49), C_tD_3 r(42)
827 w	828 s	836		C_cD_3 r(43), C_tD_3 r(38)
		795		C_cD_3 r(30), C_tD_3 r(30), NC_c s(12), CN s(10)
	700 vs	700		CC s(29), NC_t s(12), CO ib(12), NC_c s(11)
			588	CO ob(75)
568 m	570 s	574		CO ib(42), NC_t s(15), CC s(11), CN s(10)
452 w	450 m	449		CCN d(57), C_tNC_c r(20), CO ib(10)
	362 s	362		C_tNC_c d(81), CN s(11)
310 w			305	NC_c ob(21), NC_t ob(21), CC s(16), CN t(13), CO ob(10)
		239		C_tNC_c r(66), CCN d(30)
			225	CC t(86)
			181	CN t(58), NC_t t(36), NC_c ob(13), NC_t ob(13)
			166	NC_c t(88)
			158	NC_t t(56), CN t(34)
				$CD_3CON(CD_3)_2$ (D_9)
		2241		C_cD_3 as(45), C_tD_3 as(39), CD_3 as(12)
		2227		CD_3 as(83), C_tD_3 as(12)
2261 w	2260 w	2226		C_cD_3 as(50), C_tD_3 as(47)
			2225	C_tD_3 as(89)
			2224	C_cD_3 as(94)
			2222	CD_3 as(86)
		2115		C_tD_3 ss(49), C_cD_3 ss(48)
2135 w	2150 s	2114		C_cD_3 ss(49), C_tD_3 ss(49)
		2112		CD_3 ss(98)
1644 s	1642 sh	1648		CO s(77), CN s(16), CCN d(11)
1429 s	1425 m	1433		CN s(43), CO ib(23), CC s(18)

Table 5. (*continued*)

Observed* i.r.	Observed* Raman	Calculated A'	Calculated A''	Potential energy distribution†
1253 m	1245 m	1242		NC_t s(56), NC_c s(19), $C_t NC_c$ r(10)
1150 vw	1140 vw	1146		NC_c s(44), C_cD_3 sb(29), CC s(18), CO ib(11)
1086 w		1074		C_tD_3 sb(70), CD_3 sb(19)
	1069 m	1062		CD_3 sb(33), C_cD_3 sb(22), C_tD_3 sb(21), C_tD_3 ab(19)
			1061	C_cD_3 ab(44), C_tD_3 ab(38)
	1069 m	1060		C_cD_3 ab(50), C_tD_3 ab(29), CD_3 sb(10)
1059 vw			1054	C_tD_3 ab(50), C_cD_3 ab(42)
	1053 vw	1052		C_cD_3 ab(41), C_tD_3 ab(37), CD_3 sb(12)
1044 vw		1036		C_tD_3 sb(42), CD_3 sb(19)
		1029		CD_3 ab(89)
			1028	CD_3 ab(95)
			955	C_tD_3 r(36), C_cD_3 r(30)
			846	CD_3 r(47), C_cD_3 r(31). CO ob(12)
	843 m		841	C_tD_3 r(43), C_cD_3 r(23), CD_3 r(21)
829 w	830 m	836		C_cD_3 r(44), C_tD_3 r(37)
	816 m	810		CD_3 r(61)
		792		C_tD_3 r(30), C_cD_3 r(28), NC_c s(15), NC_t s(10)
	664 vs	650		CD_3 r(17), CN s(16), CC s(16), NC_t s(13), NC_c s(10)
551 w	550 m	558		CO ib(47), CC s(17), NC_t s(10)
			543	CO ob(60), CD_3 r(22)
	413 w	419		CCN d(48), C_tNC_c r(27), CD_3 r(10)
	360 s	361		C_tNC_c d(81), CN s(12)
			300	NC_c ob(23), NC_t ob(23), CN t(15), CO ob(11)
		226		C_tNC_c r(59), CCN d(36)
			178	NC_t t(53), CN t(39), NC_t ob(10), NC_c ob(10)
			170	NC_c t(65), CC t(33)
			159	CC t(59), NC_c t(29)
			153	CN t(52), NC_t t(40)

*s = strong; m = medium; w = weak; v = very; sh = shoulder.

†s = stretch; as = antisymmetric stretch; ss = symmetric stretch; ib = in-plane bend; ob = out-of-plane bend; ab = antisymmetric bend; sb = symmetric bend; r = rock; d = deformation; t = torsion; the subscripts *t* and *c* to C denote the methyl carbons attached to N in *trans* and *cis* configurations with respect to O. Only contributions of 10 or greater are included.

‡Fermi resonance corrected unperturbed value.

vibrational analyses of poly(L-alanine) [7, 9] and poly(α-amino isobutyric acid) [12] have already shown. In fact, our i.r. and Raman spectra of DMA shows two bands in this region, one at 229 (i.r.) and the other at 240 (Raman) cm^{-1}, and the agreement between our calculated values and the observed bands is quite good, including the splitting. The calculated value of CN t at 182 cm^{-1} is also in good agreement with the observed band at 186 cm^{-1} [25]. This low value is consistent with the lowering of this mode when H on N is replaced by D in the amide group [1], keeping in mind that in DMA the substitution is by a much heavier methyl group.

$CD_3CON(CH_3)_2$ (D_3)

On deuteration to CD_3(C), all the modes of this group shift down and the spectra show new bands in place of the CH_3(C) vibrations. The bands at 2260 and 2112 cm^{-1} can be assigned to CD_3(C) as and CD_3(C) ss, respectively. The predicted values from the calculation are somewhat lower because the stretch force constants transferred from D_0 were adjusted for the Fermi resonance-corrected stretch frequencies whereas we have not made any such corrections to the observed bands of D_3. The new bands observed in the spectra at about 1052, 1038, 1018, 853, 825 and 700 cm^{-1} are well assigned to CD_3(C) modes. The calculation predicts all of these with an average discrepancy of ~11 cm^{-1}, which is reasonable considering the change in anharmonicity upon deuteration. It is worth mentioning that none of the earlier normal mode calculations [13–16] predicted a mode near 853 cm^{-1}. In addition to these, some of the bands in D_0 shift, even though the modes contain no contribution ≥10% from the CH_3(C) group. For instance, the D_0 bands observed at 1660, 590 and 472 cm^{-1}, exhibit downshifts of 11, 22 and 27 cm^{-1}, which are quite reasonably predicted by our calculation, viz. 7, 25 and 29 cm^{-1}, respectively. On the other hand, the small upward shift of imide III, from 1269 to 1276 cm^{-1}, is not predicted.

$CH_3CON(CD_3)_2$ (D_6)

As in the case of D_3, it is not possible to assign the CD_3(N) s modes unambiguously unless a Fermi resonance analysis is done. Because of the several overlapping bands between 2300 and 2000 cm^{-1}, it is difficult to estimate the intensities of the bands and to do such an analysis. The calculated CD_3(N) s frequencies are unperturbed values, and therefore cannot be compared directly with the (perturbed) observed values. New bands are observed in the spectrum at 1067,

1055, 878, 841 and 828 cm^{-1}, and four of these are well assigned to $CD_3(N)$ modes. The calculation does not predict an observed Raman band at 878 cm^{-1}, but since none of the earlier normal mode calculations [13–16] did not either, this band could very well be due to some impurity in the sample. The small (less than for D_3) downward shift in imide I (from 1660 to 1654 cm^{-1}) is well predicted. The complex mixture of CN s and CH_3 ab in D_0 and D_3 is replaced in D_6 by a purer CN s (imide II) mode calculated at 1450 cm^{-1}, and an observed counterpart is found at 1449 cm^{-1}. Also, the imide III mode, at 1269 cm^{-1} in D_0, is predicted to shift down to 1242 cm^{-1} in D_6, and this mode is indeed observed at 1247 cm^{-1}. A mixed mode near 1190 cm^{-1} in D_0 is observed to shift to 1144 cm^{-1}; we calculate this mode to shift from 1199 to 1155 cm^{-1}. The direction of the shift of the 1013 cm^{-1} CH_3 r mode to 977 cm^{-1} is predicted by our calculation, although the magnitude is less satisfactorily reproduced, with the calculations giving a value of 990 cm^{-1}. This may be a result of a change in the character of this mode, from pure CH_3 r in D_0 to CH_3 r + CC s, in D_6. The shifts of the skeletal modes at 737, 590, 472 and 421 cm^{-1} to 700, 570, 450 and 362 cm^{-1}, respectively, are very well predicted. The observed downward shift of NC_c ob, from 333 cm^{-1} in D_0 to 310 cm^{-1} in D_6, is also in good agreement with the predicted shift from 329 to 305 cm^{-1}

$CD_3N(CD_3)_2$ (D_9)

The spectra of the completely deuterated molecule shows some interesting features. The downward shift of the imide I band has increased from an average of 9 cm^{-1} in the D_3 and D_6 derivatives to 16 cm^{-1}, compared to a predicted shift of 12 cm^{-1}. Imide II is predicted to shift down further, to 1433 cm^{-1}, and the observed band is indeed found to have moved down to 1429 cm^{-1}. Imide III is predicted to be at the same value as in D_6, viz. 1242 cm^{-1}; the observed band is at ~1249 cm^{-1}. The CD_3 ab, CD_3 sb, and CD_3 r modes dominate the region from 1200 to 800 cm^{-1}, with some contribution to modes even as low as 420 cm^{-1}. The downward shifts in the skeletal modes, to 664 (mixed with CD_3 r), 550 and 413 cm^{-1}, are well reproduced.

CONCLUSIONS

The present refinement of a complete SGVFF for DMA, i.e. including in-plane and out-of-plane modes, gives good agreement between observed and calculated frequencies for DMA (average discrepancy of 5.0 cm^{-1} for bands below 1700 cm^{-1}) and three of its deuterated derivatives (similar average discrepancy of 5.6 cm^{-1}). This is comparable to that achieved for our peptide force fields [1, 10], and, since the force constants are similar, opens the possibility of refining an analogous force field for the proline moiety in polypeptides and proteins.

Acknowledgements—This research was supported by National Science Foundation grants DMB-8517812 and DMR-8303610, and by the Program in Protein Structure and Design at The University of Michigan.

REFERENCES

[1] S. KRIMM and J. BANDEKAR, *Adv. Protein Chem.* **38**, 181 (1986).
[2] J. JAKEŠ and S. KRIMM, *Spectrochim. Acta* **27A**, 19 (1971).
[3] Y. ABE and S. KRIMM, *Biopolymers* **11**, 1817 (1972).
[4] W. H. MOORE and S. KRIMM, *Biopolymers* **15**, 2439 (1976).
[5] A. M. DWIVEDI and S. KRIMM, *Macromolecules* **15**, 177 (1982).
[6] W. H. MOORE and S. KRIMM, *Biopolymers* **15**, 2465 (1976).
[7] A. M. DWIVEDI and S. KRIMM, *Macromolecules* **15**, 186 (1982).
[8] J. F. RABOLT, W. H. MOORE and S. KRIMM, *Macromolecules* **10**, 1065 (1977).
[9] A. M. DWIVEDI and S. KRIMM, *Biopolymers* **23**, 923 (1984).
[10] S. KRIMM, *Biopolymers* **22**, 217 (1983).
[11] S. KRIMM and A. M. DWIVEDI, *Science* **216**, 407 (1982).
[12] A. M. DWIVEDI, S. KRIMM and B. R. MALCOLM, *Biopolymers* **23**, 2025 (1984).
[13] N. JOHNSTON, Ph.D. Thesis, University of Michigan, Ann Arbor, MI (1975).
[14] G. DURGAPRASAD, D. N. SATHYANARAYANA, C. C. PATEL, H. S. RANDHAWA, A. GOEL and C. N. R. RAO, *Spectrochim. Acta* **28A**, 2311 (1972).
[15] V. V. CHALAPATHI and K. V. RAMIAH, *Proc. Indian Acad. Sci.* **68A**, 109 (1968).
[16] C. GARRIGOU-LAGRANGE and M. FOREL, *J. Chim. phys. Physicochim. Biol.* **68**, 1329 (1971).
[17] C. GARRIGOU-LAGRANGE, C. DELOZÉ, P. BACELON, PH. COMBELAS and J. DAGANT, *J. Chim. phys. Physicochim. Biol.* **67**, 1936 (1970).
[18] J. L. KATZ and B. POST, *Acta crystallogr.* **13**, 624 (1960).
[19] T. KOJIMA, T. KIDO, H. ITOH, T. YAMANE and T. ASHIDA, *Acta crystallogr. B* **36**, 326 (1980).
[20] H. ITOH, T. YAMANE and T. ASHIDA, *Acta crystallogr. B* **34**, 2640 (1978).
[21] J. F. YAN, F. A. MOMANY, R. HOFFMANN and H. A. SCHERAGA, *J. phys. Chem.* **74**, 420 (1970).
[22] Y. SUGAWARA, A. Y. HIRAKAWA and M. TSUBOI, *J. molec. Spectrosc.* **115**, 21 (1986).
[23] T. C. CHEAM and S. KRIMM, *J. molec. Struct.*, in press.
[24] S. KRIMM and A. M. DWIVEDI, *J. Raman Spectrosc.* **12**, 133 (1982).
[25] E. D. SCHMID and E. BRODBEK, *J. molec. Struct.* **108**, 17 (1984).